

# Serine Phosphorylation Is Critical for the Activation of Ubiquitin-Specific Protease 1 and Its Interaction with WD40-Repeat Protein UAF1

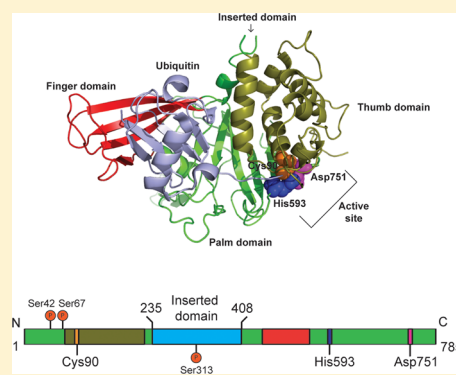
Mark A. Villamil,<sup>†</sup> Qin Liang,<sup>†</sup> Junjun Chen,<sup>†,§</sup> Yong Seok Choi,<sup>‡,||</sup> Shuyu Hou,<sup>‡</sup> Kelvin H. Lee,<sup>‡</sup> and Zhihao Zhuang<sup>\*,†</sup>

<sup>†</sup>Department of Chemistry and Biochemistry, 214A Drake Hall, University of Delaware, Newark, Delaware 19716, United States

<sup>‡</sup>Department of Chemical and Biomolecular Engineering, University of Delaware, Newark, Delaware 19716, United States

## S Supporting Information

**ABSTRACT:** Deubiquitinating enzymes (DUBs) are important for the normal function of a number of cellular processes, including transcriptional regulation, cell cycle control, and DNA damage response. The enzymatic activity of DUB is regulated by different mechanisms. DUBs in several different families are post-translationally modified by phosphorylation. Large-scale phosphoproteomic studies of human DUBs revealed that a majority of ubiquitin-specific proteases (USPs) are phosphorylated. USP1 is a prototypical DUB that requires a specific interaction with a WD40-repeat protein, UAF1, for its catalytic activity. In this study, we show that Ser313 phosphorylation in USP1 is required for its interaction with UAF1 and for the stimulation of USP1's activity. In contrast, two other known USP1 serine phosphorylations (Ser42 and Ser67) are dispensable with respect to the activity of the USP1/UAF1 complex. An S313D phosphomimetic mutation in USP1 can substitute for Ser313 phosphorylation in promoting the formation of the USP1/UAF1 complex. We further demonstrated that CDK1 is responsible for Ser313 phosphorylation, and protein phosphatase treatment of USP1 can lead to inactivation of USP1/UAF1. An inserted domain in USP1 (amino acids 235–408) was found to interact with UAF1, and this interaction is mediated by Ser313 phosphorylation. Our findings revealed an intriguing mechanism of regulating USP1 activity that combines phosphorylation of a key serine residue in USP1 and the specific interaction of USP1 with a WD40-repeat protein UAF1. The pSer313-dependent formation of the USP1/UAF1 complex points to a new approach for inhibiting USP1 activity by disrupting the interaction between the UAF1's WD40-repeat domain and the Ser313-containing phosphopeptide in USP1.



Protein ubiquitination is an important post-translational modification that regulates a multitude of cellular processes, including protein degradation, innate immunity, cell cycle control, and DNA damage response. These processes are tightly regulated by enzymes responsible for ubiquitin conjugation and deubiquitination. Ubiquitination requires the sequential action of three enzymes: ubiquitin activating enzyme (E1), ubiquitin conjugating enzyme (E2), and ubiquitin ligase (E3).<sup>1</sup> Deubiquitinating enzymes (DUBs) counteract the activity of ubiquitin ligases and provide a means of regulating the ubiquitination state of target proteins.<sup>2,3</sup> DUBs are isopeptidases that cleave the polyubiquitin chain or remove the monoubiquitin moiety from modified proteins. DUBs can be grouped into at least five families, four of which are cysteine proteases: ubiquitin C-terminal hydrolases (UCHs), ubiquitin-specific proteases (USPs), ovarian tumor (OTU) domain-containing proteins, and Machado-Joseph domain (MJD)-containing proteins.<sup>4,5</sup> A fifth family of DUBs (JAMM) consists of zinc-dependent metalloproteases. In humans, the ubiquitin-specific proteases (USPs) constitute the largest of the DUB families with close to 60 members.

USPs are typically large, multidomain enzymes with a conserved catalytic core. The USP catalytic core contains a conserved Cys-His-Asp/Asn catalytic triad. Common features of USPs are the N- and C-terminal extensions that flank the catalytic core domain. The USP terminal domains play an important role in regulating the catalytic activity of the DUB catalytic core. The terminal domains can stimulate DUB activity through either a direct interaction with the catalytic core or an allosteric mechanism. In human USP7, the C-terminal ubiquitin-like domain (UBL) is essential for both DUB activity and ubiquitin binding.<sup>6–8</sup> In Ubp15, a yeast homologue of USP7, both the N- and C-terminal domains were shown to stimulate the activity of the catalytic core.<sup>9</sup> A zinc-finger Ub-specific protease (ZnF-UBP) domain in USP5 is known to stimulate the catalytic core activity by increasing its rate of catalytic turnover.<sup>10,11</sup>

Received: June 23, 2012

Revised: October 6, 2012

Published: November 1, 2012



Besides the terminal domains, other protein factors can also stimulate the DUB activity through the formation of the complex. DUBs interact with a large number of protein factors, and a global protein interaction study has identified >700 interacting proteins for the 75 DUBs analyzed.<sup>12</sup> A number of USPs were found to have their catalytic activity stimulated by their associated proteins. In the SAGA deubiquitinating module, Sgf11 is required for the activation of Ubp8 through a direct interaction between the Ubp8 active site and a motif in Sgf11.<sup>13,14</sup> The GMP synthetase (GMPS) was found to interact with and stimulate USP7 activity through its binding to the first three UBLs in USP7 (HUBL-1–3) and promote an “on state” in USP7.<sup>6</sup> Human USP1 is stimulated by the WD40-repeat protein UAF1 (USP1-associated factor 1) through the formation of a stable complex.<sup>15,16</sup> Using probes specific for the cysteine catalytic triad residues, we recently showed that UAF1 activates USP1 by modulating its active site conformation.<sup>16</sup> It has now become clear that the catalytic activity of USPs can be regulated either intramolecularly by the domains flanking the USP catalytic core or intermolecularly by USP-interacting protein partners.

Besides the terminal extensions in the USP sequences, the USP catalytic core also commonly contains inserted domains and sequences. A bioinformatic study identified five common sites in the conserved USP catalytic core where extra sequences can be inserted.<sup>17</sup> The roles of many of the insertions remain largely unknown. A recent study of USP4 revealed that a ubiquitin-like domain embedded in the USP4 catalytic core can bind to the enzyme ubiquitin binding site located between the finger and palm–thumb domains in the catalytic core, thus inhibiting USP4 DUB activity.<sup>18</sup>

Regulation of DUB activity is critical for the ubiquitin-mediated pathways given their indispensable roles in a number of cellular pathways.<sup>5</sup> Post-translational modifications, such as phosphorylation, ubiquitination, and SUMOylation, have been reported for a large number of DUBs.<sup>19</sup> Many of these modifications were found to have an impact on DUB catalytic activity. Despite some recent progress,<sup>20,21</sup> our understanding of the regulation of DUB by post-translational modification, particularly phosphorylation, remains limited.

USP1 represents a large group of human USPs that interact with the WD40-repeat proteins. Remarkably, many human USPs were found to be associated with WD40-repeat proteins that adopt a  $\beta$ -propeller structure.<sup>12</sup> Given its widespread occurrence, the specific interaction between USPs and their cognate WD40-repeat proteins likely represents an important mechanism for regulating USP activity. To date, how USP1 and UAF1 interact and how the formation of the USP1/UAF1 complex is regulated remain largely unknown. In this study, we investigated the phosphorylation of USP1 at three different serine residues. We found that Ser313 phosphorylation plays an essential role in regulating the formation of the USP1/UAF1 complex. Mutation of Ser313 in USP1 to Ala abolished its interaction with UAF1 as revealed by pull-down and chemical cross-linking studies. A phosphomimetic mutant (S313D USP1) retained normal interaction with UAF1. Moreover, we identified an inserted domain in the USP1 catalytic core that contributes to UAF1 binding. This inserted domain harbors the Ser313 phosphorylation site and can bind to UAF1 upon phosphorylation of Ser313 or a phosphomimetic substitution. We also demonstrated that CDK1 is able to phosphorylate the isolated USP1-inserted domain and the full-length USP1 and confers the normal UAF1 interaction. Our observation revealed

a regulatory mechanism of USP1's activity in which a specific phosphorylation in USP1 and the subsequent interaction with a partner protein UAF1 exert the stimulatory effect on USP1 catalytic activity.

## ■ EXPERIMENTAL PROCEDURES

**Expression and Purification of Wild-Type and Mutant USP1 and USP1/UAF1 Complex.** USP1 and UAF1 genes were cloned into the pFastBac Dual vector (Invitrogen) for insect cell (Sf9) expression. G670A and G671A mutations were introduced into the USP1 gene to prevent proteolytic cleavage. The doubly His-tagged USP1/UAF1 complex (wild-type or mutant) was expressed and purified as previously described.<sup>16,22</sup> We also expressed the wild-type and mutant USP1/UAF1 complex consisting of six-His-tagged USP1 and untagged UAF1 in insect Sf9 cells. The infected cells were harvested 72 h post-infection. The harvested cells were washed twice with PBS buffer containing 137 mM NaCl, 2.7 mM KCl, 10 mM Na<sub>2</sub>HPO<sub>4</sub>, and 2 mM KH<sub>2</sub>PO<sub>4</sub> (pH 7.4). Cells were resuspended in lysis buffer containing 50 mM NaH<sub>2</sub>PO<sub>4</sub> (pH 8.0), 500 mM NaCl, 10 mM imidazole, 5 mM  $\beta$ -mercaptoethanol ( $\beta$ -ME), and 10% glycerol. The cells were sonicated on ice and centrifuged at 4 °C. The supernatant was incubated with Ni-NTA agarose resin (Invitrogen) at 4 °C for 1 h with constant shaking followed by extensive washing with lysis buffer. The USP1/UAF1 complex was eluted from the resin with an elution buffer containing 50 mM NaH<sub>2</sub>PO<sub>4</sub> (pH 8.0), 500 mM NaCl, 250 mM imidazole, 5 mM  $\beta$ -ME, and 10% glycerol. Protein purity was analyzed by denaturing sodium dodecyl sulfate–polyacrylamide gel electrophoresis (SDS–PAGE). Pure fractions were combined and subjected to buffer exchange against a storage buffer consisting of 50 mM Tris (pH 8.0), 100 mM NaCl, 2 mM DTT, and 10% glycerol.

The expression and purification of USP1 alone were similar to those of USP1/UAF1. The Sf9 cells were infected with virus that harbors the USP1 gene. Wild-type or mutant USP1 was purified following the protocol described above.

The USP1 inserted domain (USP1<sub>ID</sub>, amino acids 235–408) was cloned into the pGEX vector (GE Healthcare) using the BamHI and XhoI restriction sites. Point mutations S313A and S313D were introduced into USP1<sub>ID</sub> by the QuikChange protocol. The constructs of wild-type and mutant USP1<sub>ID</sub> were transformed into *Escherichia coli* BL21(DE3) cells for protein expression. Cells were grown in LB medium with 100  $\mu$ g/mL ampicillin at 37 °C to an OD<sub>600</sub> of 0.4; the temperature was reduced to 16 °C, and cells were induced with 0.2 mM IPTG. Cells were grown overnight and harvested the next day. Cells were resuspended in a lysis buffer containing 50 mM Tris (pH 7.5), 200 mM NaCl, 1 mM DTT, and 10% glycerol. The cells were sonicated on ice and centrifuged at 4 °C. The supernatant was incubated with glutathione resin (GE Healthcare) for 1 h at 4 °C with constant agitation. Following extensive wash with the lysis buffer, protein was eluted with an elution buffer containing 50 mM Tris (pH 7.5), 200 mM NaCl, 1 mM DTT, 10% glycerol, and 10 mM reduced glutathione. Eluted protein was dialyzed against a buffer containing 50 mM Tris (pH 7.5), 5 mM NaCl, 1 mM DTT, and 10% glycerol overnight. The protein was further purified on a HiTrap SP FF column (GE Healthcare). Pure fractions were collected, concentrated, and buffer exchanged against 50 mM Tris (pH 7.5), 100 mM NaCl, 1 mM DTT, and 10% glycerol.

**Steady-State Kinetic Measurements.** The *in vitro* deubiquitinating activities of the wild-type and mutant USP1

and USP1/UAF1 complex were tested using a fluorogenic substrate, ubiquitin 7-amino-4-methylcoumarin (Ub-AMC). Ub-AMC was incubated in a reaction buffer containing 50 mM HEPES (pH 7.8), 0.5 mM EDTA, 0.1 mg/mL BSA, and 1 mM DTT at 25 °C. The fluorescence signal was measured using a Fluoromax-4 fluorescence spectrophotometer following the addition of enzyme. The rate was determined by following the fluorescence at 440 nm with 355 nm excitation. The initial rate was plotted against substrate concentration from 100 nM to 3  $\mu$ M. The steady-state rate constants were determined by fitting the initial rates to the Michaelis–Menten equation  $V = (V_{\max}[S])/([S] + K_m)$  using GraphPad Prism (GraphPad Software).  $k_{\text{cat}}$  was determined by dividing  $V_{\max}$  by the total enzyme concentration used in the assay.

**Identification of Phosphorylation Sites by Mass Spectrometry.** The USP1/UAF1 sample was reduced with 100 mM DTT followed by alkylation with 150 mM iodoacetamide and then digested with trypsin (Promega, Madison, WI) at 37 °C overnight. Samples were acidified with formic acid to end enzymatic activity and dried in a SpeedVac centrifugal vacuum concentrator (Thermo Scientific, Waltham, MA). For dephosphorylation, the USP1/UAF1 sample was treated with protein phosphatase 1 (New England Biolabs, Ipswich, MA) according to the manufacturer's instruction before trypsin digestion.

Samples were resuspended in mobile phase A (2% acetonitrile and 0.1% formic acid), and five replicates were injected into an UltiMate 3000 instrument (Dionex, Sunnyvale, CA) equipped with a C18 column (Acclaim PepMap100, 75  $\mu$ m inside diameter  $\times$  150 mm, 3  $\mu$ m, 100 Å, Dionex) for reverse phase liquid chromatography. The peptides eluted over a 66 min gradient from 2 to 50% mobile phase B (98% acetonitrile and 0.1% formic acid) with a flow rate of 250 nL/min. Eluting peptides were ionized by a NanoSpray II source (AB Sciex, Framingham, MA) into a 4000 Q TRAP (AB Sciex) hybrid triple quadrupole linear ion trap mass spectrometer. Predefined  $m/z$  450–1800 MS survey scans were acquired; up to six dynamically excluded precursors were selected for MS/MS ( $m/z$  100–2000). The Mascot search software was used to assign MS/MS spectra considering variable modifications of carbamidomethyl (C), deamidated (NQ), oxidation (M), phospho (ST), and phospho (Y). The peptide mass tolerance was set to  $\pm 1.2$  Da, and the fragment mass tolerance was set to  $\pm 0.6$  Da. A maximum of one missed cleavage per peptide was allowed, and we considered only assignments made at >95% confidence corresponding to a Mascot cutoff of 33 in this study.

The relative quantification of peptide and protein phosphorylation was conducted by following the strategy described by Steen and co-workers.<sup>23</sup> Briefly, the intensities of phosphorylated or unphosphorylated peptides were normalized on the basis of six peptides (NVEAIGLLAAOK, WLLFDDSEVK, ALDFTDSQENEK, GVVENYNDEEVSIR, WAISQFASVER, and CLECESLTER) from the same protein. Then, all relevant data from missed cleavages or different charge states of the peptides were aggregated. The relative abundance was calculated on the basis of the intensity of the target peptide divided by the median intensity of the six peptides listed above. The relative phosphorylation stoichiometry was quantified by dividing the relative abundance of a phosphopeptide by the relative abundance of all variations (phosphorylated and unphosphorylated) of the same peptide.

**Native Gel Analysis of the Wild-Type and Mutant USP1/UAF1 Complex.** An 8% native gel containing no SDS

was prepared and used with a running buffer containing 25 mM Tris, 190 mM glycine, and 1 mM DTT adjusted to pH 8.0. Running buffer, the native gel, and gel running equipment were cooled to 4 °C before being used. USP1, UAF1, and USP1/UAF1 samples were diluted to a volume of 30  $\mu$ L and a final concentration of 2  $\mu$ M. To the sample was added 6  $\mu$ L of loading dye, and the final solution contained 0.5% Coomassie G, 50 mM 6-aminocaproic acid, and 10 mM Bis-Tris (pH 7.0). The sample was loaded onto the gel, and electrophoresis was conducted at 4 °C and 90 V until the loading dye ran off the native gel. The gel was visualized with Coomassie blue staining.

**Phosphatase Treatment of the USP1/UAF1 Complex.** The USP1/UAF1 complex was treated with protein phosphatase 1 (PP1) (New England Biolabs) following the manufacturer's instructions. Aliquots of the treated sample were taken at 30, 60, 120, and 960 min. The aliquots were tested for activity using Ub-AMC as a substrate.

**Chemical Cross-Linking of the USP1/UAF1 Complex.** The wild-type and mutant USP1/UAF1 complex were dialyzed in a buffer containing 50 mM Tris (pH 7.5), 100 mM NaCl, 10% glycerol, and 1 mM TCEP overnight at 4 °C using Slide-A-Lyzer dialysis cassettes (Thermo Scientific). The protein concentration was determined following dialysis. The cross-linker 1,8-bis(maleimido)diethylene glycol or BM(PEG)<sub>2</sub> (Thermo Scientific) was dissolved in dimethyl sulfoxide (DMSO). A total enzyme concentration of 2.0  $\mu$ M was used for the cross-linking reaction. The samples were mixed with 200  $\mu$ M BM(PEG)<sub>2</sub> (or DMSO in the control reaction). Samples were incubated on ice for 1 h after the addition of the cross-linker. After 1 h, the reaction was quenched with 0.5 M DTT. Samples were then analyzed on an 8% denaturing SDS–PAGE gel and visualized by Coomassie blue staining.

For cross-linking of individually purified wild-type and mutant USP1 and UAF1 using BM(PEG)<sub>2</sub>, each of the protein samples was dialyzed in a buffer containing 50 mM Tris (pH 7.5), 100 mM NaCl, 10% glycerol, and 1 mM TCEP overnight at 4 °C using Slide-A-Lyzer dialysis cassettes. The concentrations of the protein samples were determined following the dialysis. USP1, USP1(S313D), USP1(S313A), USP1(S67D), and USP(S67A) were individually incubated with UAF1 at a 1:1 stoichiometry with a final concentration of 2  $\mu$ M on ice for 2 h. After incubation, 200  $\mu$ M BM(PEG)<sub>2</sub> was added to the solutions for cross-linking. The reaction solutions were incubated for 1 h on ice. The reaction was quenched with the addition of 0.5 M DTT. Samples were analyzed on an 8% denaturing SDS–PAGE gel.

Mass spectrometry was performed to confirm that the cross-linked band contained USP1 and UAF1. The USP1/UAF1 complex was treated with the cross-linker BM(PEG)<sub>2</sub> as described above. The treated sample was run on an 8% denaturing SDS–PAGE gel, and the cross-linked band was excised, treated, and digested with trypsin as described above. The digested sample was resuspended in mobile phase A (2% acetonitrile and 0.1% formic acid) and injected into an UltiMate 3000 instrument equipped with a C18 column for reverse phase liquid chromatography. The peptides eluted over a 66 min gradient from 2 to 50% mobile phase B (98% acetonitrile and 0.1% formic acid). Eluting peptides were ionized by a NanoSpray II source (AB Sciex) into a 4000 Q TRAP (AB Sciex), hybrid triple quadrupole linear ion trap mass spectrometer. The Mascot search software was used to assign MS/MS spectra considering variable modifications of carbamidomethyl (C), deamidated (NQ), oxidation (M), phospho



**Table 1. Kinetic Properties of the Wild-Type and Mutant USP1/UAF1 Complexes**

enzyme	$k_{\text{cat}}$ ( $\text{s}^{-1}$ )	$K_{\text{m}}$ (nM)	$k_{\text{cat}}/K_{\text{m}}$ ( $\text{M}^{-1} \text{s}^{-1}$ )	$\alpha$ -fold decrease in $k_{\text{cat}}/K_{\text{m}}$
USP1/UAF1	$0.096 \pm 0.005$	$380 \pm 130$	$2.5 \times 10^5$	
USP1(S42A)/UAF1	$0.081 \pm 0.001$	$752 \pm 40$	$1.1 \times 10^5$	2.3
USP1(S42D)/UAF1	$0.089 \pm 0.008$	$740 \pm 170$	$1.2 \times 10^5$	2.1
USP1(S67A)/UAF1	$0.070 \pm 0.003$	$712 \pm 64$	$1.0 \times 10^5$	2.5
USP1(S67D)/UAF1	$0.068 \pm 0.002$	$515 \pm 50$	$1.3 \times 10^5$	1.9
USP1(S313A)/UAF1	$0.001 \pm 0.0001$	$934 \pm 290$	$1.1 \times 10^3$	227
USP1(S313D)/UAF1	$0.084 \pm 0.005$	$332 \pm 62$	$2.5 \times 10^5$	1.0

(ST), and phospho (Y). With a 75 ppm precursor error tolerance, the MS/MS fragment tolerance was set to  $\pm 0.3$  Da. A maximum of one missed cleavage per peptide was allowed, and a >95% confidence interval was used for assignment.

**Western Blotting against USP1 and UAF1.** The USP1/UAF1 complex subjected to chemical cross-linking was resolved on an 8% SDS–PAGE gel and transferred to a nitrocellulose membrane. The membrane was blocked with TBS buffer containing 3% BSA and 0.05% Tween and incubated with primary antibodies against USP1 (Abcam) or HA (Sigma-Aldrich). HRP-conjugated anti-rabbit (Bio-Rad) or anti-mouse IgG (Sigma-Aldrich) antibodies were used as secondary antibodies. Images were generated by chemiluminescence (Pierce ECL).

**Pull-Down Experiments.** N-Terminally GST-tagged wild-type USP1\_ID, USP1(S313A)\_ID, and USP1(S313D)\_ID were incubated with glutathione resin at 4 °C for 1 h. UAF1 was then added to the resin and the mixture incubated for 1 h. The solutions were centrifuged to remove the supernatant. The resin was washed extensively with PBS buffer at 4 °C. A solution containing 10 mM reduced glutathione was used to elute the protein from glutathione resin. Both the elution solution and the wash solution were analyzed on a denaturing 10% SDS–PAGE gel.

In a reverse pull-down experiment, UAF1 was used as the bait protein. N-Terminally HA-tagged UAF1 was incubated with HA resin (EZview Red Anti-HA Affinity Gel, Sigma) at 4 °C for 1 h. USP1\_ID, USP1(S313A)\_ID, and USP1(S313D)\_ID were incubated individually with the HA resin bound with UAF1. After incubation at 4 °C for 1 h, the resin was extensively washed with PBS buffer at 4 °C. The washed resin was then heat denatured at 100 °C for 5 min. The proteins were eluted from the resin and analyzed on an 8% denaturing SDS–PAGE gel.

In a separate pull-down experiment, N-terminally GST-tagged wild-type USP1\_ID (5  $\mu\text{M}$ ) was first treated with CDK1 or CK2 (New England Biolabs) according to the manufacturer's instructions at 30 °C for 2 h. The treated USP1\_ID samples were incubated with glutathione resin for 1 h at 4 °C. UAF1 was then added to the individual USP1\_ID samples and incubated at 4 °C for 1 h. Following incubation, the resins were washed extensively with PBS buffer at 4 °C for 30 min and centrifuged to remove the supernatant. A solution containing 10 mM reduced glutathione was used to elute the protein from GST resin. Both the elution and wash solutions were analyzed on a denaturing 10% SDS–PAGE gel.

**Assay Activity of the Reconstituted USP1/UAF1 Complex.** Individually purified wild-type USP1 (2.5  $\mu\text{M}$ ) was incubated with CDK1 at 30 °C for up to 2 h following the manufacturer's instructions. Both kinase-treated and untreated USP1 samples were incubated with UAF1 at a molar ratio of 1:1 at 37 °C for 30 min. The DUB activity of the incubation

mixture was assayed as described above using Ub-AMC as a substrate. The specific activity was calculated by dividing the reaction rate by the molar concentration of USP1 in the assay solution.

## RESULTS

**Identification of USP1 Phosphorylation Sites by Mass Spectrometry.** The USP1/UAF1 complex purified from insect cells was reduced with 100 mM dithiothreitol, alkylated with 150 mM iodoacetamide, and then digested with trypsin at 37 °C overnight. The resulting peptides were analyzed by mass spectrometry. Two serine phosphorylation sites, Ser313 and Ser67, in USP1 were identified. The detected phosphopeptides are ATSDTLEpS<sup>313</sup>PPKIIPK and ASEIDQVVPAAQSp-S<sup>67</sup>PINCEKR (Figure S1 of the Supporting Information). Our findings are in accord with previous proteomic analyses showing that Ser67 and Ser313 of USP1 were phosphorylated in human cells.<sup>24,25</sup> Ser42 was previously reported to be phosphorylated<sup>26</sup> but was not detected in our analysis.

**Mutational Analysis of the Phosphorylated USP1 Residues.** To assess the effect of serine phosphorylation on USP1's catalytic activity, the identified serine residues were mutated to either Ala or Asp. The alanine mutation abolished phosphorylation of the targeted residue, while the aspartate mutant acted as a phosphomimetic. The wild-type or mutant USP1 was coexpressed with UAF1 (both proteins contained a six-His tag) in insect cells and purified using a nickel affinity column. The purified wild-type USP1/UAF1 protein showed a  $k_{\text{cat}}/K_{\text{m}}$  that was 35-fold higher than that of USP1 purified alone as previously reported.<sup>16,22</sup>

Phosphorylation-deficient and phosphomimetic mutations at three different serine residues, Ser42, Ser67, and Ser313, in USP1 were generated. The mutant USP1 was coexpressed and purified with UAF1 using a nickel affinity column as described for the wild-type protein. The mutant USP1 purified with UAF1 was assayed for DUB activity using Ub-AMC as a substrate. The steady-state rate constants were determined (Table 1). Among the three Ser to Ala mutations, only the USP1(S313A)/UAF1 complex showed a large decrease in its catalytic efficiency. A 227-fold decrease in  $k_{\text{cat}}/K_{\text{m}}$  was evident upon comparison to that of the wild-type USP1/UAF1 complex. The decrease in catalytic activity is primarily a  $k_{\text{cat}}$  effect, with a 96-fold decrease in the value of  $k_{\text{cat}}$ . In marked contrast, the USP1(S42A)/UAF1 and USP1(S67A)/UAF1 complexes showed little change in catalytic activity, with 2.3- and 2.5-fold decreases in  $k_{\text{cat}}/K_{\text{m}}$ , respectively (Table 1).

The catalytic activity of the corresponding phosphomimetic mutant complexes, USP1(S313D)/UAF1, USP1(S42D)/UAF1, and USP1(S67D)/UAF1, was measured. Different from the USP1(S313A)/UAF1 complex, the USP1(S313D)/UAF1 complex retained normal catalytic activity [ $k_{\text{cat}}/K_{\text{m}} = 2.5 \times 10^5 \text{ M}^{-1} \text{ s}^{-1}$  (Table 1)]. Both USP1(S42D)/UAF1 and

USP1(S67D)/UAF1 complexes demonstrated a level of catalytic efficiency similar to that of the wild-type enzyme with  $k_{\text{cat}}/K_m$  values of  $1.2 \times 10^5$  and  $1.3 \times 10^5 \text{ M}^{-1} \text{ s}^{-1}$ , respectively.

The catalytic activity of the wild-type and mutant USP1 alone was measured. Unlike the USP1/UAF1 complex, USP1(S313A) exhibited a catalytic efficiency ( $k_{\text{cat}}/K_m = 4.8 \times 10^3 \text{ M}^{-1} \text{ s}^{-1}$ ) similar to that of the wild type and USP1(S313D) (Table 2). Little change in  $k_{\text{cat}}/K_m$  was observed for the USP1(S42A), USP1(S42D), USP1(S67A), and USP1(S67D) mutants.

**Table 2. Kinetic Properties of Wild-Type and Mutant USP1**

enzyme	$k_{\text{cat}}$ ( $\text{s}^{-1}$ )	$K_m$ (nM)	$k_{\text{cat}}/K_m$ ( $\text{M}^{-1} \text{ s}^{-1}$ )
USP1	$0.0040 \pm 0.0002$	$570 \pm 39$	$7.0 \times 10^3$
USP1(S42A)	$0.0035 \pm 0.0002$	$641 \pm 98$	$5.5 \times 10^3$
USP1(S42D)	$0.0044 \pm 0.0003$	$763 \pm 148$	$5.8 \times 10^3$
USP1(S67A)	$0.0037 \pm 0.0002$	$478 \pm 75$	$7.7 \times 10^3$
USP1(S67D)	$0.0033 \pm 0.0002$	$684 \pm 89$	$4.8 \times 10^3$
USP1(S313A)	$0.0032 \pm 0.0003$	$660 \pm 58$	$4.8 \times 10^3$
USP1(S313D)	$0.0042 \pm 0.0001$	$519 \pm 39$	$8.1 \times 10^3$

**Native Gel Electrophoresis of the Wild-Type and Mutant USP1/UAF1 Complexes.** To assess whether the stability of the USP1/UAF1 complex was affected by the Ser313 to Ala mutation in USP1, the wild-type and mutant USP/UAF1 complexes were analyzed using native gel electrophoresis. As shown in Figure 1A, three discrete bands corresponding to the USP1/UAF1 complex and the individual UAF1 and USP1 proteins were detected in native gel electrophoresis and Coomassie blue staining. For the USP1-(S313A)/UAF1 complex, no band corresponding to the USP1/UAF1 complex was detected. Instead, individual UAF1 and USP1 bands were detected. For the USP1(S313D)/UAF1 complex, a band similar to that of the wild-type USP1/UAF1 complex was detected.

To confirm the identity of the bands on the native gel, we performed Western blotting using anti-USP1 and anti-HA tag antibodies. The anti-USP1 and anti-HA tag antibodies were specific and allowed the detection of USP1 and the N-terminally HA-tagged UAF1, respectively (in Figure 1, compare panels A–C). For the wild-type USP1/UAF1 complex, a single band corresponding to the complex was detected with both antibodies (Figure 1B,C), confirming the presence of both USP1 and UAF1 polypeptides in the native gel band assigned as the USP1/UAF1 complex. The same was observed for the USP1(S313D)/UAF1 complex, in agreement with the Coomassie staining result (Figure 1A). In marked contrast, a band corresponding to the USP1/UAF1 complex was absent for the USP1(S313A)/UAF1 complex in both the Coomassie blue-stained gel (Figure 1A) and the Western blotting gels (Figure 1B,C). Instead, individual USP1(S313A) and UAF1 bands were detected. These results suggest that USP1 Ser313 phosphorylation is required for formation of the complex between USP1 and UAF1. A phosphomimetic USP1(S313D) mutant can substitute Ser313 phosphorylation in promoting formation of the USP1/UAF1 complex.

**Assessing the Interaction of Wild-Type and Mutant USP1 with UAF1.** To confirm that the interaction between USP1 and UAF1 is mediated by USP1 Ser313 phosphorylation, six-His-tagged USP1 was coexpressed with untagged UAF1 in insect cells. After the cells were lysed, the cell lysate was passed

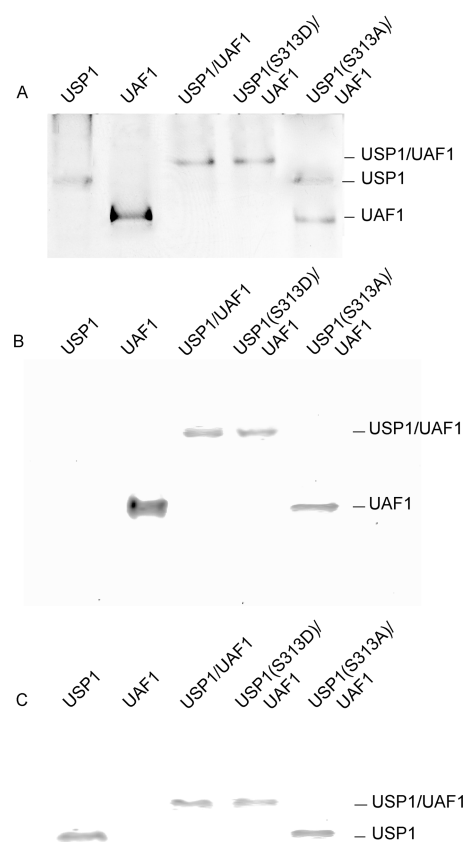


**Figure 1.** Native PAGE analysis of the wild-type and mutant USP1/UAF1 complexes in comparison to individual UAF1 and USP1 proteins. (A) Native gel of USP1, UAF1, and wild-type USP1/UAF1, USP1(S313D)/UAF1, and USP1(S313A)/UAF1 complexes. The protein bands were visualized by Coomassie blue staining. (B) Western blot of USP1, UAF1, and wild-type USP1/UAF1, USP1-(S313D)/UAF1, and USP1(S313A)/UAF1 complexes separated on a native gel using an antibody against the HA tag on UAF1. (C) Western blot of USP1, UAF1, and wild-type USP1/UAF1, USP1-(S313D)/UAF1, and USP1(S313A)/UAF1 complexes separated on a native gel using an antibody against USP1.

through a nickel affinity column. After a stringent wash, the column was eluted with a 100 mM imidazole solution. For the wild-type six-His-tagged USP1 coexpressed with untagged UAF1, the eluted fractions contained both USP1 and UAF1, suggesting that wild-type USP1 can form a stable complex with UAF1 when expressed in insect cells. In marked contrast, when six-His-tagged USP1(S313A) was coexpressed with untagged UAF1 in insect cells, although the mutant USP1 was retained on the nickel affinity column as observed for wild-type USP1, no UAF1 was retained on the column. A parallel experiment with USP1(S313D) showed a result similar to that for wild-type USP1 in that a USP1(S313D)/UAF1 complex was retained on the nickel column. This agreed with the native gel electrophoresis study suggesting that mutation of Ser313 of USP1 to Ala prevented formation of the USP1/UAF1 complex, while the USP1(S313D) mutant retains a normal ability to form a complex with UAF1. We also assessed the USP1(S42A), USP1(S42D), USP1(S67A), and USP1(S67D) mutants in a

similar experiment. In all cases, the USP1 mutants can be purified as a complex with UAF1.

The catalytic activity of the singly six-His-tagged USP1/UAF1 complex that contained wild-type or mutant USP1 was assessed. As shown in Table S1 of the Supporting Information, the steady-state kinetic constants of the USP1(S42A)/UAF1, USP1(S42D)/UAF1, USP1(S67A)/UAF1, USP1(S67D)/UAF1, and USP1(S313D)/UAF1 complexes are close to those of the wild-type USP1/UAF1 complex. Their  $k_{cat}$  and  $K_m$  values are also similar to those of the corresponding doubly six-His-tagged USP1/UAF1 complex (Table 1). In contrast, USP1(S313A) without associated UAF1 demonstrated greatly reduced catalytic efficiency (Table S1 of the Supporting Information).

**Phosphatase Treatment of the USP1/UAF1 Complex Inactivates the Enzyme Complex.** Given that reversible phosphorylation is a common mechanism for regulating the activity of the protein complex, we next asked the question of whether dephosphorylation of USP1 can lead to inactivation of the USP1/UAF1 complex. We demonstrated using mass spectrometry that treatment of the purified wild-type USP1/UAF1 complex with PP1 effectively removed the phosphate group from Ser313 and Ser67. Relative abundances of 0.644 and 0.523 were determined for the Ser313 and Ser67 phosphopeptides, respectively (Figure S2 of the Supporting Information). Following the PP1 treatment, the pSer313 and pSer67 phosphopeptides were no longer detected, indicating an effective dephosphorylation of USP1 at these two positions. The DUB activity of the USP1/UAF1 complex treated with PP1 was measured. In a control experiment, the USP1/UAF1 complex treated with phosphatase buffer did not result in an appreciable decrease in the activity of the USP1/UAF1 complex. When the USP1/UAF1 complex was treated with PP1, a large decrease in its activity was observed. After a 30 min treatment, 4% of the activity for the treated USP1/UAF1 complex remain. After an overnight treatment, only 1% of the activity remained (Figure S3 of the Supporting Information).

**Chemical Cross-Linking of the USP1/UAF1 Complex.** Chemical cross-linking has been used successfully to demonstrate the formation of the protein complexes.<sup>27–29</sup> BM(PEG)<sub>2</sub> is a bifunctional thiol-specific cross-linker that has been used for cross-linking cysteine residues. The wild-type and mutant six-His-tagged USP1 that was coexpressed and purified with the six-His-tagged UAF1 from insect cells was subjected to a chemical cross-linking study. The protein sample was incubated with BM(PEG)<sub>2</sub> in a solution containing 50 mM Tris (pH 7.5), 100 mM NaCl, 10% glycerol, and 1 mM TCEP for 60 min. The cross-linking products were analyzed by denaturing SDS-PAGE. As shown in Figure 2, there was an observed new protein band close to 212 kDa after cross-linking. There was a clear reduction in the intensity of the USP1 and UAF1 bands, suggesting that the new band is due to cross-linking of the USP1 and UAF1 bands. The presence of USP1 and UAF1 in the cross-linked species was shown by Western blotting analysis (Figure 3). To further confirm the identity of the cross-linked band, the cross-linked protein species was subjected to tandem mass spectrometry analysis. Using the search engine Mascot, we confirmed the presence of both USP1 and UAF1 in the cross-linked band (Table S2 and Figure S4 of the Supporting Information).

A similar cross-linking pattern was observed for the USP1(S313D)/UAF1 complex (Figure 2). In contrast, USP1(S313A) was not cross-linked to UAF1 as indicated by the lack

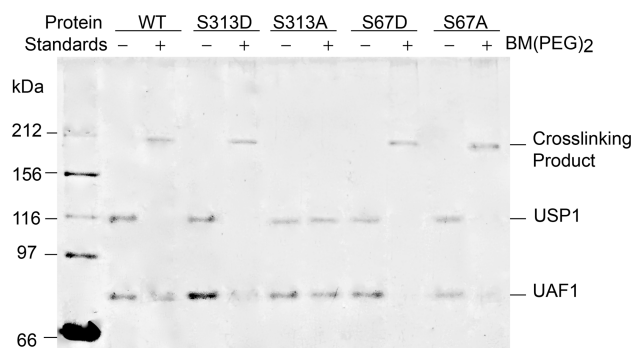


**Figure 2.** Chemical cross-linking of the wild-type and mutant USP1/UAF1 complexes using BM(PEG)<sub>2</sub>. The reaction mixtures were separated on an 8% denaturing SDS-PAGE gel and stained with Coomassie blue. For the wild-type (WT) USP1/UAF1, USP1(S313D)/UAF1, USP1(S67D)/UAF1, and USP1(S67A)/UAF1 complexes, a cross-linked species was observed with a molecular mass close to 212 kDa. No cross-linking product was observed for the USP1(S313A)/UAF1 complex.

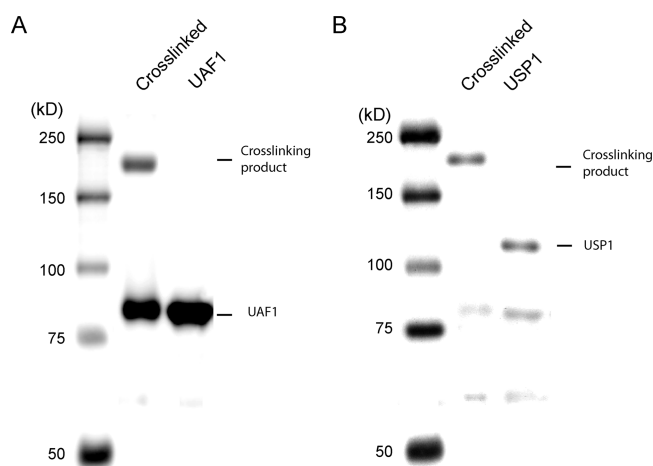


**Figure 3.** Western blotting analysis of the USP1/UAF1 complex cross-linked with BM(PEG)<sub>2</sub>. (A) Western blot against the cross-linking product and UAF1 using the anti-HA antibody. UAF1 contained a HA tag at its N-terminus. (B) Western blot against the cross-linking product and USP1 using an anti-USP1 antibody.

of the high-molecular weight band observed for the wild-type USP1 and USP1(S313D)/UAF1 complexes. As a comparison, we also subjected the USP1(S67D) and USP1(S67A) mutants to chemical cross-linking analysis. In both cases, a cross-linked band close to 212 kDa was detected (Figure 2), suggesting that formation of a complex between the USP1(S67D) and USP1(S67A) mutants and UAF1 was normal. The results of the cross-linking experiments agreed well with those of the native gel electrophoresis and affinity purification studies described above.

In another set of chemical cross-linking experiments, individually purified wild-type or mutant USP1 was mixed with UAF1. The protein mixture was incubated with BM(PEG)<sub>2</sub>. Interestingly, no band was detected for the cross-linked complex of wild-type USP1 (Figure 4). Nonetheless, the cross-linked band for USP1(S313D), but not for USP1(S313A), with UAF1 was detected. The difference in the cross-linking pattern between the copurified USP1/UAF1 complex and individually purified USP1 suggests that Ser313



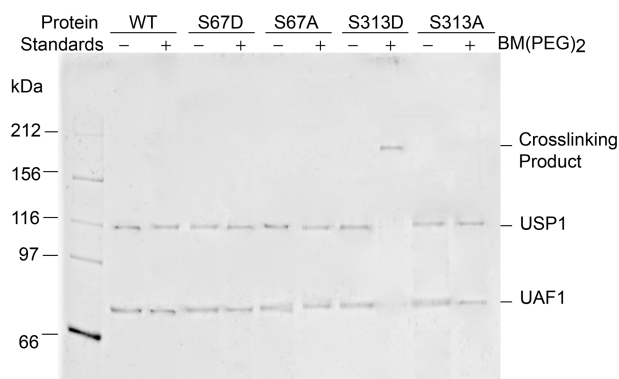


**Figure 4.** Individually purified wild-type and mutant USP1 is subjected to cross-linking with UAF1 using BM(PEG)<sub>2</sub>. The reaction mixtures were separated on an 8% denaturing SDS–PAGE gel and stained with Coomassie blue. No cross-linking product was observed for the wild-type (WT) USP1/UAF1, USP1(S67D)/UAF1, USP1(S67A)/UAF1, and USP1(S313A)/UAF1 complexes. A cross-linked species with a molecular weight close to 212 kDa was observed for the USP1-(S313D)/UAF1 complex.

likely undergoes dephosphorylation when being individually expressed and purified from insect cells.

**Probing the Interaction between UAF1 and the USP1 Inserted Domain (USP1\_ID) by a Pull-Down Experiment.** USP1, like many other USPs, is a multiple-domain protein (Figure 5). Ser313 is located in an inserted domain

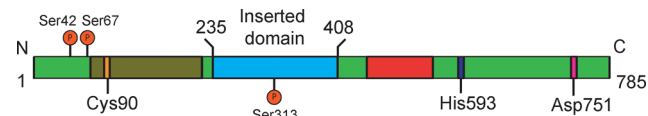


**Figure 5.** Schematic representation of the USP1 domain structure. The USP1 inserted domain (USP1\_ID, colored blue) is located between residues 235 and 408. The catalytic residues Cys90, His593, and Asp751 are indicated. The palm, thumb, and finger domains are colored green, olive, and red, respectively. The three phosphorylation sites (Ser42, Ser67, and Ser313) are indicated.

encompassing 173 amino acid residues between positions 235 and 408. To determine whether this domain contributes to the interaction between USP1 and UAF1, a truncated USP1 (amino acids 235–408) (USP1\_ID) with a N-terminal GST fusion was generated for the pull-down assay with UAF1. The

protein was expressed in *E. coli* cells and purified with a glutathione affinity column. USP1(S313A)\_ID and USP1-(S313D)\_ID fused with GST were also generated. In the pull-down assay, wild-type or mutant GST-USP1\_ID was used as a bait to pull down UAF1. As shown in Figure 6, only USP1(S313D)\_ID as bait pulled down UAF1. No UAF1 was pulled down by either wild-type USP1 or USP1(S313A)\_ID. As a control, UAF1 was incubated with glutathione resin bound with GST, and no UAF1 was pulled down.

In a reverse pull-down experiment, an N-terminal HA-tagged UAF1 was used as the bait protein and incubated with a resin coated with the anti-HA antibody. USP1\_ID, USP1(S313A)\_ID, and USP1(S313D)\_ID were individually introduced and incubated with the resin charged with UAF1. Following a stringent wash, the captured protein was heat denatured and analyzed on a 10% denaturing SDS–PAGE gel. As shown in Figure 7, UAF1 was able to pull down USP1(S313D)\_ID, but not USP1\_ID or USP1(S313A)\_ID, in accord with the pull-down assay results using USP1\_ID as bait (Figure 6). The results from the pull-down experiments support a specific interaction between USP1\_ID and UAF1 mediated through Ser313 phosphorylation.

**Phosphorylation of USP1 by CDK1.** Given that Ser313 of USP1 is located in a CDK1 phosphorylation sequence, we next tested whether CDK1 is responsible for its phosphorylation. Wild type USP1\_ID with an N-terminal GST tag was treated with either CDK1 or a control kinase, CK2, at 30 °C for 2 h. The treated USP1\_ID samples were then subjected to the pull-down assay with UAF1 as described above. As shown in Figure 8, USP1\_ID treated with CDK1 pulled down UAF1 efficiently. In contrast, the CK2-treated USP1\_ID was not able to pull down UAF1.

To demonstrate that CDK1 also phosphorylates full-length USP1, individually purified USP1 was treated with CDK1 and incubated with UAF1 at a 1:1 molar ratio at 37 °C for 15 min. The mixture was then assayed for DUB activity using Ub-AMC as a substrate, and the measured specific activity was compared to that of the copurified USP1/UAF1 complex (treated as 100%). Treatment of USP1 with CDK1 led to a large increase in activity upon incubation with UAF1 as compared to untreated USP1 (Figure 9). The activity of USP1 after treatment with CDK1 for 2 h showed approximately 40% specific activity relative to the copurified USP1/UAF1 complex. As a comparison, USP1(S313D) after incubation with UAF1 showed approximately 83% activity. This observation suggests

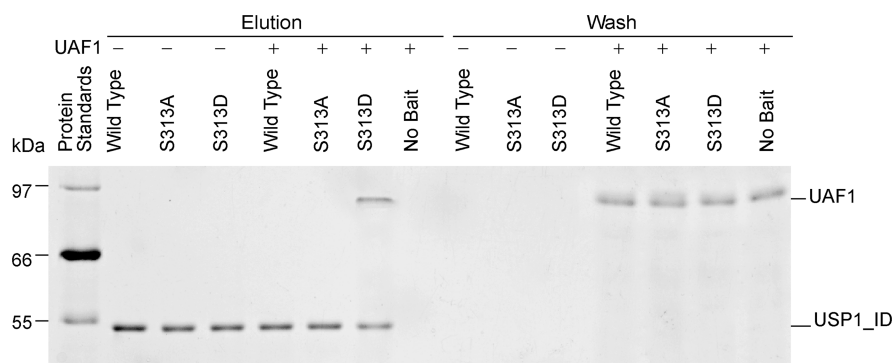


**Figure 6.** Pull down of UAF1 by wild-type and mutant USP1\_ID. Wild-type USP1\_ID, USP1(S313A)\_ID, and USP1(S313D)\_ID with an N-terminal GST tag bound to the glutathione resin were used as bait. Both the eluted protein solutions and the wash solutions were analyzed on a denaturing SDS–PAGE gel and detected by Coomassie blue staining. Only USP1(S313D)\_ID was found to pull down UAF1 efficiently.

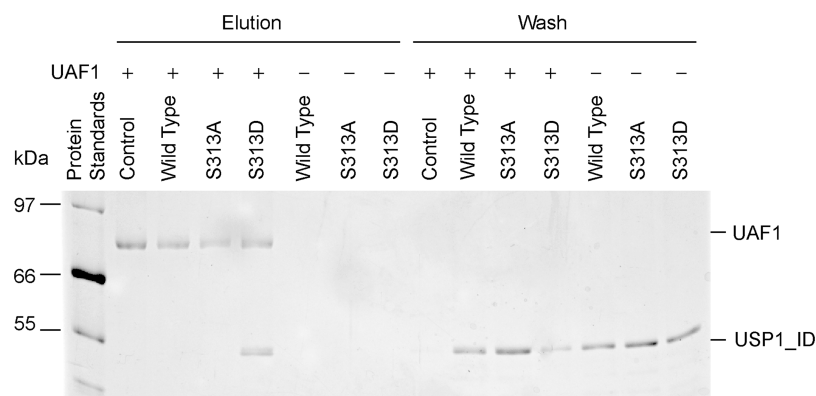


**Figure 7.** Pull down of wild-type and mutant USP1\_ID by UAF1. UAF1 with an N-terminal HA tag was used as bait for the pull-down assay. Both the eluted protein solutions and the wash solutions were analyzed on a denaturing SDS-PAGE gel and detected by Coomassie blue staining. USP1(S313D)\_ID, but not the wild type or USP1(S313A)\_ID, was able to be pulled down by UAF1.

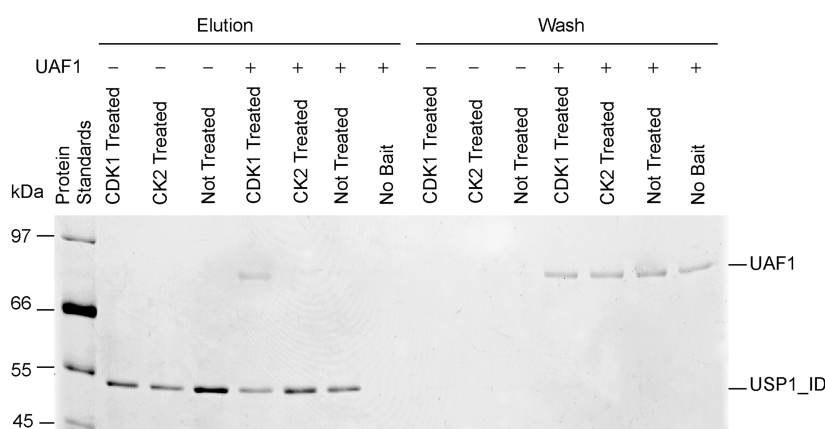


**Figure 8.** CDK1-treated USP1\_ID is able to pull down UAF1. Wild-type USP1\_ID with an N-terminal GST tag was treated with either CDK1 or CK2. Treated USP1\_ID was bound to glutathione resin and used as bait for the pull-down assay. Both the eluted protein solutions and the wash solutions were analyzed on a denaturing SDS-PAGE gel and detected by Coomassie blue staining. USP1\_ID treated with CDK1 allowed efficient pull down of UAF1, while CK2-treated USP1\_ID did not pull down UAF1.

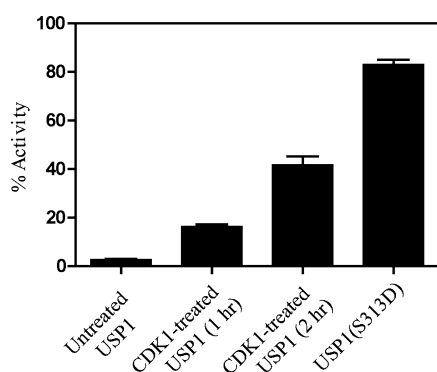


**Figure 9.** Treatment of full-length USP1 with CDK1 showed stimulation in DUB activity upon incubation with UAF1. Treated full-length USP1 was compared to USP1(S313D) in the experiment. The specific activity of the USP1/UAF1 complex copurified from insect cells was treated as 100%.

that complete phosphorylation of Ser313 was not achieved under the kinase reaction condition.

## DISCUSSION

The important roles of DUB in a myriad of cellular processes require stringent control of the DUB activity in cells. DUBs in several different families were reported to be post-translation-

ally modified, including phosphorylation, ubiquitination, and SUMOylation.<sup>3,19,30</sup> Large-scale phosphoproteomic analyses of human DUBs revealed that 37 of 55 ubiquitin-specific proteases (USPs) are phosphorylated.<sup>24,31–33</sup> Human CYLD, a ubiquitin-specific protease involved in cylindromatosis, is phosphorylated at Ser418, which negatively affects the DUB activity of the enzyme.<sup>34,35</sup> Another well-known example of DUB phosphorylation is A20, an ovarian tumor domain (OTU)-containing protease. A20 was found to be phosphorylated at Ser381 by kinase IKK $\beta$ . Phosphorylation of A20 leads to increased DUB activity toward NEMO.<sup>36</sup> Human USP7 was reported to be phosphorylated at Ser18 and Ser963.<sup>7</sup> Among them, USP7 Ser18 phosphorylation was found to be required for its cellular stability, which in turn contributes to Mdm2 stabilization and p53 downregulation.<sup>37</sup>

Although many DUBs were reported to be phosphorylated, detailed biochemical and structural studies of this common modification of DUBs are limited. A recent study of the human deubiquitinase DUBA provided a detailed understanding of the stimulatory effect of Ser177 phosphorylation on DUBA's catalytic activity.<sup>20</sup> Notably, the phosphate group on Ser177 in DUBA helps to bring two distant regions of the enzyme around the C-terminal tail of the bound ubiquitin and thus contributes to ubiquitin binding and catalysis.



In this study, we uncovered a novel regulatory mechanism of human USP1 through phosphorylation of Ser313. Remarkably, the stimulatory effect of USP1 Ser313 phosphorylation requires UAF1, a WD40-repeat protein that interacts with USP1. USP1 Ser313 phosphorylation promotes formation of the complex between USP1 and UAF1. A phosphomimetic mutant, USP1(S313D), retains its normal ability to interact with UAF1 and stimulates the USP1 DUB activity to a level comparable to that of the wild-type enzyme. We observed a slightly lower  $k_{\text{cat}}$  for the USP1(S313D)/UAF1 complex ( $0.084 \text{ s}^{-1}$ ) compared to that of the wild-type USP1/UAF1 complex ( $0.096 \text{ s}^{-1}$ ). This can be understood in light of the fact that phosphomimetics may not fully recapitulate the effect of native phosphorylation as has been previously shown for kinases and DNA glycosylase.<sup>38–40</sup>

We previously reported that UAF1 stimulates the catalytic activity of USP1 through an allosteric mechanism by modulating the USP1 active site.<sup>16</sup> To gain further insight into the mechanism of Ser313 phosphorylation-mediated activation of USP1, we generated a modeled structure of the USP1 catalytic core using SWISS-MODEL (<http://swissmodel.expasy.org/>)<sup>41,42</sup> (see Figure 10). The USP7 structure was used

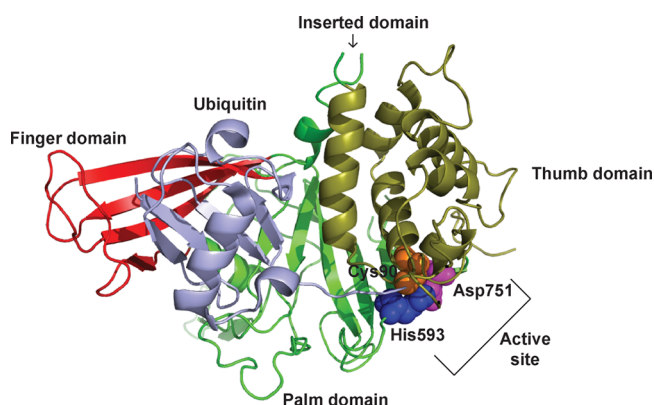


**Figure 10.** Modeled USP1 catalytic core structure. The catalytic core was modeled using USP7 as a template. The USP1 palm, thumb, and finger domains are colored green, olive, and red, respectively. Ubiquitin is built into the modeled structure by superimposing USP1 onto the structure of the USP7–Ub complex. The site of the inserted domain is indicated by an arrow. The catalytic triad residues are labeled.

as a template for the modeling.<sup>43</sup> The human USP1 catalytic core contains an inserted domain (ID) between amino acids 235 and 408, in which Ser313 is located. The modeled USP1 catalytic core structure does not contain the inserted domain. Nonetheless, the predicted site of insertion between amino acids 235 and 408 is distant from the USP1 catalytic site marked by the cysteine triad. Although it is not yet known how UAF1 binds to USP1\_ID in the absence of a structure of the complex, the large separation of the inserted domain from the catalytic site of USP1 suggests that the effect of UAF1 on USP1 catalytic activity may be mediated through a long-range allosteric mechanism. This is in accord with our previous finding that UAF1 stimulates the catalytic activity of USP1 allosterically by modulating the USP1 active site.<sup>16</sup> However, we cannot rule out a possible direct interaction between UAF1 and the USP1 active site given the large size of the UAF1 eight-blade  $\beta$ -propeller structure and a large C-terminal extension in

UAF1 that was recently reported to contain discrete domains participating in direct protein–protein interaction.<sup>44</sup>

In USP1, Ser313 is located in a consensus sequence (TLES<sup>313</sup>PPK) for cyclin-dependent kinase. A previous study reported that CDK1 is responsible for phosphorylation of Ser313 of USP1 in human cells.<sup>45</sup> Interestingly, the Ser313 phosphorylation site is also located in a degron mapped to amino acids 307–330 for APC/C<sup>Cdh1</sup>-mediated USP1 degradation.<sup>46</sup> Phosphorylation of Ser313 was found to be important for USP1's stability during mitosis. It was suggested that phosphorylation of USP1 at Ser313 serves as an interface for the association of USP1 with UAF1. Our findings support this notion. It is conceivable that the association of UAF1 with USP1 masks the APC/C<sup>Cdh1</sup> degron, thus promoting the stability of USP1. Given that the degron is required for direct interaction with Cdh1 in the APC/C ubiquitin ligase complex, direct competition between UAF1 and Cdh1 for this region in USP1 is possible. Notably Cdh1, like UAF1, is a WD40-repeat protein, although no sequence similarity is found between these two proteins. This represents an intriguing mechanism of regulating the stability and activity of USP1 through its interaction with two different WD40-repeat proteins. It will be of interest to assess the effect of phosphorylation of Ser313 of USP1 on its interaction with Cdh1.

Besides allosteric regulation of enzyme activity, phosphorylation of serine/threonine residues has been implicated in mediating formation of protein complexes, particularly through phosphoserine/phosphothreonine-binding domains. The WD40 domain represents an important class of pSer/pThr-binding domains.<sup>47</sup> One of the better-studied WD40-repeat protein is the SCF ubiquitin ligase  $\beta$ -TrCP1.  $\beta$ -TrCP1 contains a WD40 domain that folds into a seven-blade  $\beta$ -propeller structure and binds to substrate protein  $\beta$ -catenin, a component of the Wnt signaling pathway.<sup>48–50</sup> Structural determination of the phosphorylated  $\beta$ -catenin peptide binding to the WD40 domain of  $\beta$ -TrCP1 revealed that the peptide binds to the top face of the  $\beta$ -propeller through extensive hydrogen bonding and electrostatic interaction between the phosphate group of phosphorylated serines (Ser33 and Ser37) in  $\beta$ -catenin and the WD40-repeat motif.<sup>51</sup> Besides the phosphoserine peptide, the phosphothreonine peptide is also known to bind to the WD40-repeat domain. SCF<sup>Cdc4</sup> ubiquitin ligase has been shown to bind a Cdc4 phosphodegron (CPD) peptide corresponding to the nine amino acids of human cyclin E.<sup>52</sup> The CPD peptide adopts an extended conformation and binds the second blade of the  $\beta$ -propeller with its N-terminus oriented toward the central pore of the WD40 domain. The pThr residue is engaged in a network of hydrogen bonding and electrostatic interactions with the WD40 domain residues.

The phosphopeptide binding to the WD40-repeat domain in the SCF ubiquitin ligase complex contributes to the ubiquitination reaction mainly through increasing the effective concentration of the targeted lysine residue at the E2 active site.<sup>53</sup> In the case of the USP1 pSer313 peptide binding to the WD40 domain of UAF1, the phosphorylation of Ser313 of USP1 plays a more complex role in activating the deubiquitination activity. Ser313 phosphorylation not only is required for the tight association between USP1 and UAF1 but also plays a role in relaying the long-range allostery induced by the binding of UAF1.

The USP1/UAF1 complex is an important player in two major DNA damage response pathways, i.e., translesion DNA synthesis and the Fanconi anemia pathway. It thus represents a

promising therapeutic target for cancer therapy. We recently demonstrated that selective USP1/UAF1 complex inhibitors identified through high-throughput screening sensitized non-small cell lung cancer cells to killing by DNA-damaging agent cisplatin.<sup>22</sup> More recently, USP1 was reported to deubiquitinate ID (inhibitors of DNA binding) proteins that inhibit cell differentiation and maintain stem cell fate in osteosarcoma.<sup>54</sup> This observation also suggested USP1 as a potential target for differential therapy. Our finding of the pSer313-dependent formation of the USP1/UAF1 complex points to a new approach of inhibiting USP1 activity. By disrupting formation of the complex, particularly the interaction between the WD40-repeat domain and USP1 phosphopeptide, we can inhibit the activation of USP1 in cells. Considerable success in developing peptidomimetics and small molecules that disrupt phosphorylation-dependent protein interaction has been reported, including STAT3 inhibitors that target the pTyr-binding Src-homology 2 (SH2) domain.<sup>55</sup>

WD40-repeat domains represent one of the largest groups of protein interaction domains found in the human genome, with more than 250 WD40-repeat domain-containing proteins.<sup>56</sup> Because of their important roles in regulating enzymes such as ubiquitin ligases and DUBs, there is great promise in developing new therapeutics by targeting the WD40-repeat domain. Indeed, a recent high-throughput screening identified a small molecule, SCF-I2, as an allosteric inhibitor of SCF<sup>Cdc4</sup>.<sup>57</sup> Another study identified a series of small molecule enhancers of rapamycin that inhibited SCF<sup>Met30</sup> ubiquitin ligase using a yeast-based screen.<sup>58</sup> Intriguingly, SCF-I2 inhibits SCF<sup>Cdc4</sup> by inserting itself between the  $\beta$ -strands of two blades of the Cdc4 WD40 propeller domain, which is 25 Å from the point at which the substrate phosphopeptide binds. These findings raised an exciting possibility of inhibiting the binding of the phosphopeptide to the WD40-repeat domain by allosteric inhibitors. Given the divergence of sequence among the human WD40-repeat domains, a selective inhibition against the USP–WD40-repeat protein complex should be an achievable goal.

## ■ ASSOCIATED CONTENT

### ■ Supporting Information

Tables S1 and S2 and Figures S1–S4. This material is available free of charge via the Internet at <http://pubs.acs.org>.

## ■ AUTHOR INFORMATION

### Corresponding Author

\*Phone: (302) 831-8940. E-mail: [zzhuang@udel.edu](mailto:zzhuang@udel.edu).

### Present Addresses

<sup>§</sup>Institute for Bioscience and Biotechnology Research, University of Maryland College Park, 9600 Gudelsky Drive, Rockville, MD 20850.

<sup>||</sup>College of Pharmacy, Dankook University, Cheonan-Si, Chungnam 330-714, South Korea.

### Funding

This work was supported in part by a grant from the National Institutes of Health (NIH) to Z.Z. (R01GM097468) and in part by the NIH-funded Delaware INBRE program (5P20RR016472-12).

### Notes

The authors declare no competing financial interest.

## ■ ACKNOWLEDGMENTS

We thank Leila Choe for technical assistance with mass spectrometry analysis.

## ■ ABBREVIATIONS

DUB, deubiquitinating enzyme; USP, ubiquitin-specific protease; UAF1, USP1-associated factor 1;  $\beta$ -ME,  $\beta$ -mercaptoethanol; DTT, dithiothreitol; Ub-AMC, ubiquitin-7-amino-4-methylcoumarin; USP1\_ID, USP1 inserted domain; CDK1, cyclin-dependent kinase 1; CK2, casein kinase 2

## ■ REFERENCES

- (1) Pickart, C. M. (2001) Mechanisms underlying ubiquitination. *Annu. Rev. Biochem.* 70, 503–533.
- (2) Amerik, A. Y., and Hochstrasser, M. (2004) Mechanism and function of deubiquitinating enzymes. *Biochim. Biophys. Acta* 1695, 189–207.
- (3) Reyes-Turcu, F. E., Ventii, K. H., and Wilkinson, K. D. (2009) Regulation and cellular roles of ubiquitin-specific deubiquitinating enzymes. *Annu. Rev. Biochem.* 78, 363–397.
- (4) Nijman, S. M., Luna-Vargas, M. P., Velds, A., Brummelkamp, T. R., Dirac, A. M., Sixma, T. K., and Bernards, R. (2005) A genomic and functional inventory of deubiquitinating enzymes. *Cell* 123, 773–786.
- (5) Komander, D., Clague, M. J., and Urbe, S. (2009) Breaking the chains: Structure and function of the deubiquitinases. *Nat. Rev. Mol. Cell Biol.* 10, 550–563.
- (6) Faesen, A. C., Dirac, A. M., Shanmugham, A., Ovaa, H., Perrakis, A., and Sixma, T. K. (2011) Mechanism of USP7/HAUSP activation by its C-terminal ubiquitin-like domain and allosteric regulation by GMP-synthetase. *Mol. Cell* 44, 147–159.
- (7) Fernandez-Montalvan, A., Bouwmeester, T., Joberty, G., Mader, R., Mahnke, M., Pierrat, B., Schlaeppli, J. M., Worpenberg, S., and Gerhart, B. (2007) Biochemical characterization of USP7 reveals post-translational modification sites and structural requirements for substrate processing and subcellular localization. *FEBS J.* 274, 4256–4270.
- (8) Ma, J., Martin, J. D., Xue, Y., Lor, L. A., Kennedy-Wilson, K. M., Sinnamon, R. H., Ho, T. F., Zhang, G., Schwartz, B., Tummino, P. J., and Lai, Z. (2010) C-terminal region of USP7/HAUSP is critical for deubiquitination activity and contains a second mdm2/p53 binding site. *Arch. Biochem. Biophys.* 503, 207–212.
- (9) Bozza, W. P., and Zhuang, Z. (2011) Biochemical characterization of a multidomain deubiquitinating enzyme Ubp15 and the regulatory role of its terminal domains. *Biochemistry* 50, 6423–6432.
- (10) Reyes-Turcu, F. E., Horton, J. R., Mullally, J. E., Heroux, A., Cheng, X., and Wilkinson, K. D. (2006) The ubiquitin binding domain ZnF UBP recognizes the C-terminal diglycine motif of unanchored ubiquitin. *Cell* 124, 1197–1208.
- (11) Stein, R. L., Chen, Z., and Melandri, F. (1995) Kinetic studies of isopeptidase T: Modulation of peptidase activity by ubiquitin. *Biochemistry* 34, 12616–12623.
- (12) Sowa, M. E., Bennett, E. J., Gygi, S. P., and Harper, J. W. (2009) Defining the human deubiquitinating enzyme interaction landscape. *Cell* 138, 389–403.
- (13) Kohler, A., Zimmerman, E., Schneider, M., Hurt, E., and Zheng, N. (2010) Structural basis for assembly and activation of the heterotetrameric SAGA histone H2B deubiquitinase module. *Cell* 141, 606–617.
- (14) Samara, N. L., Datta, A. B., Berndsen, C. E., Zhang, X., Yao, T., Cohen, R. E., and Wolberger, C. (2010) Structural insights into the assembly and function of the SAGA deubiquitinating module. *Science* 328, 1025–1029.
- (15) Cohn, M. A., Kowal, P., Yang, K., Haas, W., Huang, T. T., Gygi, S. P., and D'Andrea, A. D. (2007) A UAF1-containing multisubunit protein complex regulates the Fanconi anemia pathway. *Mol. Cell* 28, 786–797.

- (16) Villamil, M. A., Chen, J., Liang, Q., and Zhuang, Z. (2012) A Noncanonical Cysteine Protease USP1 Is Activated through Active Site Modulation by USP1-Associated Factor 1. *Biochemistry* 51, 2829–2839.
- (17) Ye, Y., Scheel, H., Hofmann, K., and Komander, D. (2009) Dissection of USP catalytic domains reveals five common insertion points. *Mol. Biosyst.* 5, 1797–1808.
- (18) Luna-Vargas, M. P., Faesen, A. C., van Dijk, W. J., Rape, M., Fish, A., and Sixma, T. K. (2011) Ubiquitin-specific protease 4 is inhibited by its ubiquitin-like domain. *EMBO Rep.* 12, 365–372.
- (19) Kessler, B. M., and Edelman, M. J. (2011) PTMs in conversation: Activity and function of deubiquitinating enzymes regulated via post-translational modifications. *Cell Biochem. Biophys.* 60, 21–38.
- (20) Huang, O. W., Ma, X., Yin, J., Flinders, J., Maurer, T., Kayagaki, N., Phung, Q., Bosanac, I., Arnott, D., Dixit, V. M., Hymowitz, S. G., Starovasnik, M. A., and Cochran, A. G. (2012) Phosphorylation-dependent activity of the deubiquitinase DUBA. *Nat. Struct. Mol. Biol.* 19, 171–175.
- (21) Edelman, M. J., Kramer, H. B., Altun, M., and Kessler, B. M. (2010) Post-translational modification of the deubiquitinating enzyme otubain 1 modulates active RhoA levels and susceptibility to *Yersinia* invasion. *FEBS J.* 277, 2515–2530.
- (22) Chen, J., Dexheimer, T. S., Ai, Y., Liang, Q., Villamil, M. A., Inglese, J., Maloney, D. J., Jadhav, A., Simeonov, A., and Zhuang, Z. (2011) Selective and Cell-Active Inhibitors of the USP1/UAF1 Deubiquitinase Complex Reverse Cisplatin Resistance in Non-small Cell Lung Cancer Cells. *Chem. Biol.* 18, 1390–1400.
- (23) Steen, H., Jebanathirajah, J. A., Springer, M., and Kirschner, M. W. (2005) Stable isotope-free relative and absolute quantitation of protein phosphorylation stoichiometry by MS. *Proc. Natl. Acad. Sci. U.S.A.* 102, 3948–3953.
- (24) Dephoure, N., Zhou, C., Villen, J., Beausoleil, S. A., Bakalarski, C. E., Elledge, S. J., and Gygi, S. P. (2008) A quantitative atlas of mitotic phosphorylation. *Proc. Natl. Acad. Sci. U.S.A.* 105, 10762–10767.
- (25) Gauci, S., Helbig, A. O., Slijper, M., Krijgsvelde, J., Heck, A. J., and Mohammed, S. (2009) Lys-N and trypsin cover complementary parts of the phosphoproteome in a refined SCX-based approach. *Anal. Chem.* 81, 4493–4501.
- (26) Matsuoka, S., Ballif, B. A., Smogorzewska, A., McDonald, E. R., III, Hurov, K. E., Luo, J., Bakalarski, C. E., Zhao, Z., Solimini, N., Lerenthal, Y., Shiloh, Y., Gygi, S. P., and Elledge, S. J. (2007) ATM and ATR substrate analysis reveals extensive protein networks responsive to DNA damage. *Science* 316, 1160–1166.
- (27) Wilkins, B. J., Daggett, K. A., and Cropp, T. A. (2008) Peptide mass fingerprinting using isotopically encoded photo-crosslinking amino acids. *Mol. Biosyst.* 4, 934–936.
- (28) Kalkhof, S., Ihling, C., Mechtler, K., and Sinz, A. (2005) Chemical cross-linking and high-performance Fourier transform ion cyclotron resonance mass spectrometry for protein interaction analysis: Application to a calmodulin/target peptide complex. *Anal. Chem.* 77, 495–503.
- (29) Xi, J., Zhang, Z., Zhuang, Z., Yang, J., Spiering, M. M., Hammes, G. G., and Benkovic, S. J. (2005) Interaction between the T4 helicase loading protein (gp59) and the DNA polymerase (gp43): Unlocking of the gp59-gp43-DNA complex to initiate assembly of a fully functional replisome. *Biochemistry* 44, 7747–7756.
- (30) Lopez-Otin, C., and Hunter, T. (2010) The regulatory crosstalk between kinases and proteases in cancer. *Nat. Rev. Cancer* 10, 278–292.
- (31) Olsen, J. V., Blagoev, B., Gnäd, F., Macek, B., Kumar, C., Mortensen, P., and Mann, M. (2006) Global, in vivo, and site-specific phosphorylation dynamics in signaling networks. *Cell* 127, 635–648.
- (32) Diella, F., Gould, C. M., Chica, C., Via, A., and Gibson, T. J. (2008) PhosphoELM: A database of phosphorylation sites—update 2008. *Nucleic Acids Res.* 36, D240–D244.
- (33) Gnäd, F., Ren, S., Cox, J., Olsen, J. V., Macek, B., Orosi, M., and Mann, M. (2007) PHOSIDA (phosphorylation site database): Management, structural and evolutionary investigation, and prediction of phosphosites. *Genome Biol.* 8, R250.
- (34) Reiley, W., Zhang, M., Wu, X., Granger, E., and Sun, S. C. (2005) Regulation of the deubiquitinating enzyme CYLD by I $\kappa$ B kinase  $\gamma$ -dependent phosphorylation. *Mol. Cell. Biol.* 25, 3886–3895.
- (35) Hutt, J. E., Shen, R. R., Abbott, D. W., Zhou, A. Y., Sprott, K. M., Asara, J. M., Hahn, W. C., and Cantley, L. C. (2009) Phosphorylation of the tumor suppressor CYLD by the breast cancer oncogene IKK $\epsilon$  promotes cell transformation. *Mol. Cell* 34, 461–472.
- (36) Hutt, J. E., Turk, B. E., Asara, J. M., Ma, A., Cantley, L. C., and Abbott, D. W. (2007) I $\kappa$ B kinase  $\beta$  phosphorylates the K63 deubiquitinase A20 to cause feedback inhibition of the NF- $\kappa$ B pathway. *Mol. Cell. Biol.* 27, 7451–7461.
- (37) Khoronenkova, S. V., Dianova, I. I., Ternette, N., Kessler, B. M., Parsons, J. L., and Dianov, G. L. (2012) ATM-dependent down-regulation of USP7/HAUSP by PPM1G activates p53 response to DNA damage. *Mol. Cell* 45, 801–813.
- (38) Ma, X., Helgason, E., Phung, Q. T., Quan, C. L., Iyer, R. S., Lee, M. W., Bowman, K. K., Starovasnik, M. A., and Dueber, E. C. (2012) Molecular basis of Tank-binding kinase 1 activation by trans-autophosphorylation. *Proc. Natl. Acad. Sci. U.S.A.* 109, 9378–9383.
- (39) Park, C. H., Choi, B. H., Jeong, M. W., Kim, S., Kim, W., Song, Y. S., and Kim, K. T. (2011) Protein kinase C $\delta$  regulates vaccinia-related kinase 1 in DNA damage-induced apoptosis. *Mol. Biol. Cell* 22, 1398–1408.
- (40) Sidorenko, V. S., Grollman, A. P., Jaruga, P., Dizdaroglu, M., and Zharkov, D. O. (2009) Substrate specificity and excision kinetics of natural polymorphic variants and phosphomimetic mutants of human 8-oxoguanine-DNA glycosylase. *FEBS J.* 276, 5149–5162.
- (41) Bordoli, L., Kiefer, F., Arnold, K., Benkert, P., Battey, J., and Schwede, T. (2009) Protein structure homology modeling using SWISS-MODEL workspace. *Nat. Protoc.* 4, 1–13.
- (42) Kiefer, F., Arnold, K., Kunzli, M., Bordoli, L., and Schwede, T. (2009) The SWISS-MODEL Repository and associated resources. *Nucleic Acids Res.* 37, D387–D392.
- (43) Hu, M., Li, P., Li, M., Li, W., Yao, T., Wu, J. W., Gu, W., Cohen, R. E., and Shi, Y. (2002) Crystal structure of a UBP-family deubiquitinating enzyme in isolation and in complex with ubiquitin aldehyde. *Cell* 111, 1041–1054.
- (44) Yang, K., Moldovan, G. L., Vinciguerra, P., Murai, J., Takeda, S., and D'Andrea, A. D. (2011) Regulation of the Fanconi anemia pathway by a SUMO-like delivery network. *Genes Dev.* 25, 1847–1858.
- (45) Cotto-Rios, X. M., Jones, M. J., and Huang, T. T. (2011) Insights into phosphorylation-dependent mechanisms regulating USP1 protein stability during the cell cycle. *Cell Cycle* 10, 4009–4016.
- (46) Cotto-Rios, X. M., Jones, M. J., Busino, L., Pagano, M., and Huang, T. T. (2011) APC/CCdh1-dependent proteolysis of USP1 regulates the response to UV-mediated DNA damage. *J. Cell Biol.* 194, 177–186.
- (47) Yaffe, M. B., and Elia, A. E. (2001) Phosphoserine/threonine-binding domains. *Curr. Opin. Cell Biol.* 13, 131–138.
- (48) Hart, M., Concordet, J. P., Lassot, I., Albert, I., del los Santos, R., Durand, H., Perret, C., Rubinfeld, B., Margottin, F., Benarous, R., and Polakis, P. (1999) The F-box protein  $\beta$ -TrCP associates with phosphorylated  $\beta$ -catenin and regulates its activity in the cell. *Curr. Biol.* 9, 207–210.
- (49) Liu, C., Kato, Y., Zhang, Z., Do, V. M., Yankner, B. A., and He, X. (1999)  $\beta$ -Trcp couples  $\beta$ -catenin phosphorylation-degradation and regulates *Xenopus* axis formation. *Proc. Natl. Acad. Sci. U.S.A.* 96, 6273–6278.
- (50) Kitagawa, M., Hatakeyama, S., Shirane, M., Matsumoto, M., Ishida, N., Hattori, K., Nakamichi, I., Kikuchi, A., and Nakayama, K. (1999) An F-box protein, FWD1, mediates ubiquitin-dependent proteolysis of  $\beta$ -catenin. *EMBO J.* 18, 2401–2410.
- (51) Wu, G., Xu, G., Schulman, B. A., Jeffrey, P. D., Harper, J. W., and Pavletich, N. P. (2003) Structure of a  $\beta$ -TrCP1-Skp1- $\beta$ -catenin complex: Destruction motif binding and lysine specificity of the SCF( $\beta$ -TrCP1) ubiquitin ligase. *Mol. Cell* 11, 1445–1456.



- (52) Orlicky, S., Tang, X., Willems, A., Tyers, M., and Sicheri, F. (2003) Structural basis for phosphodependent substrate selection and orientation by the SCFCdc4 ubiquitin ligase. *Cell* 112, 243–256.
- (53) Zheng, N., Schulman, B. A., Song, L., Miller, J. J., Jeffrey, P. D., Wang, P., Chu, C., Koepp, D. M., Elledge, S. J., Pagano, M., Conaway, R. C., Conaway, J. W., Harper, J. W., and Pavletich, N. P. (2002) Structure of the Cul1-Rbx1-Skp1-F boxSkp2 SCF ubiquitin ligase complex. *Nature* 416, 703–709.
- (54) Williams, S. A., Maecker, H. L., French, D. M., Liu, J., Gregg, A., Silverstein, L. B., Cao, T. C., Carano, R. A., and Dixit, V. M. (2011) USP1 deubiquitinates ID proteins to preserve a mesenchymal stem cell program in osteosarcoma. *Cell* 146, 918–930.
- (55) Yap, J. L., Cao, X., Vanommeslaeghe, K., Jung, K. Y., Peddaboina, C., Wilder, P. T., Nan, A., MacKerell, A. D., Jr., Smythe, W. R., and Fletcher, S. (2012) Relaxation of the rigid backbone of an oligoamide-foldamer-based  $\alpha$ -helix mimetic: Identification of potent Bcl-xL inhibitors. *Org. Biomol. Chem.* 10, 2928–2933.
- (56) Lydeard, J. R., and Harper, J. W. (2010) Inhibitors for E3 ubiquitin ligases. *Nat. Biotechnol.* 28, 682–684.
- (57) Orlicky, S., Tang, X., Neduva, V., Elowe, N., Brown, E. D., Sicheri, F., and Tyers, M. (2010) An allosteric inhibitor of substrate recognition by the SCF(Cdc4) ubiquitin ligase. *Nat. Biotechnol.* 28, 733–737.
- (58) Aghajan, M., Jonai, N., Flick, K., Fu, F., Luo, M., Cai, X., Ouni, I., Pierce, N., Tang, X., Lomenick, B., Damoiseaux, R., Hao, R., Del Moral, P. M., Verma, R., Li, Y., Li, C., Houk, K. N., Jung, M. E., Zheng, N., Huang, L., Deshaies, R. J., Kaiser, P., and Huang, J. (2010) Chemical genetics screen for enhancers of rapamycin identifies a specific inhibitor of an SCF family E3 ubiquitin ligase. *Nat. Biotechnol.* 28, 738–742.